

Ligand Substitution from the (η^5 -DMP)Mn(CO)₂(Solv) [DMP = 2,5-dimethylpyrrole, Solv = solvent] Complexes: To Ring Slip or Not to Ring Slip?

Bert H. G. Swennenhuis,[†] Ross Poland,[‡] Wai Yip Fan,[§] Donald J. Darensbourg,^{*,‡} and Ashfaq A. Bengali^{*,†}

[†]Department of Chemistry, Texas A&M University at Qatar, Doha, Qatar, [‡]Department of Chemistry, Texas A&M University, College Station, Texas 77843-3255, and [§]Department of Chemistry, National University of Singapore, 3 Science Drive, Singapore 117543

Received June 3, 2010

The mechanism and energetics of the displacement of solvent from photolytically generated (η^5 -DMP)Mn(CO)₂(Solv) complexes has been studied [DMP = 2,5-dimethylpyrrole, Solv = solvent]. Rate enhancement relative to the η^5 -cyclopentadienyl (Cp) system is not observed in the displacement of weakly bound solvents. The bond dissociation enthalpies obtained from the kinetic analysis are in good agreement with the values obtained by detailed density functional theory (DFT) calculations. The results indicate that for both the Cp and the DMP based systems the displacement of weakly bound solvents proceeds by a dissociative or I_d mechanism. This is in sharp contrast to CO displacement from (η^5 -DMP)Mn(CO)₃, which is known to proceed by an associative mechanism by way of an η^3 ring slip intermediate. The associative substitution pathway only becomes competitive with the dissociative channel when the Mn-Solv bond dissociation enthalpy is more than 33 kcal/mol.

Introduction

The mechanism of ligand substitution reactions from transition metal containing organometallic complexes remains an important area of research.¹ The primary motivation for these studies comes from the ability of such complexes to promote both stoichiometric and catalytic transformations of organic compounds.² Most often, the active metal containing species is generated by ligand loss from a precursor complex followed by binding of a substrate molecule.³ Fundamental information regarding the energetics and mechanism of ligand substitution is therefore desirable. Ligand substitution from metal complexes containing the η^5 -cyclopentadienyl (Cp) ligand is of particular interest since highly reactive reduced hapticity complexes can be generated as intermediates in the reactions.⁴ The incoming ligand can then occupy the resulting open coordination site on the metal thereby providing a low energy

pathway for the substitution reaction.⁵ For example, the associative substitution of a CO ligand from CpM(CO)₂ [M = Co, Rh, Ir] is thought to occur by way of a “ring slipped” intermediate formed by a $\eta^5 \rightarrow \eta^3$ haptotropic shift of the Cp ligand.⁶ The ring slip mechanism was supported by observation of the unusually high associative lability of the (η^5 -Indenyl)Rh(CO)₂ complex.⁷ The traditional explanation for this high reactivity was attributed to the “indenyl effect” whereby the η^3 indenyl intermediate is stabilized by the re-aromatization of the benzene ring (Scheme 1). Recent theoretical studies have provided an alternate explanation for this effect.⁸ These calculations have suggested that the origin of the indenyl effect is based on both the weaker η^5 binding of the indenyl ligand to the metal center and to a lower energy for the η^3 intermediate relative to Cp.

More pertinent to the current study, other systems also appear to exhibit this type of rate enhancement. For example, while CpMn(CO)₃ is thermally inert to CO substitution, its *N*-heterocycle analogue (η^5 -C₄H₄N)Mn(CO)₃ reacts readily with phosphines and phosphites to form (η^5 -C₄H₄N)Mn(CO)₂(PR₃) complexes.⁹ The pyrrole complex was estimated to react almost 10⁸ times faster than the cyclopentadienyl

*To whom correspondence should be addressed. E-mail: ashfaq.bengali@qatar.tamu.edu (A.A.B.), djdarens@mail.chem.tamu.edu (D.J.D.).

(1) (a) Darensbourg, D. J. *Adv. Organomet. Chem.* **1982**, *21*, 113. (b) Basolo, F. *Coord. Chem. Rev.* **1982**, *43*, 7. (c) Howell, J. A. S.; Bukinshaw, P. M. *Chem. Rev.* **1983**, *83*, 557.

(2) (a) Herrmann, W. A.; Cornils, B. *Applied Homogeneous Catalysis with Organometallic Compounds*; Wiley-VCH: Berlin, 2002. (b) Masters, C. *Homogeneous Transition-Metal Catalysis: A Gentle Art*; Chapman Hall: London, 1980. (c) Parshall, G. W.; Ittel, S. D. *Homogeneous Catalysis – The Application and Chemistry of Catalysis by Soluble Transition-Metal Complexes*; John Wiley and Sons: New York, 1980. (d) Cornils, B.; Herrmann, W. A. *J. Catal.* **2003**, *216*, 23.

(3) Heaton, B., Ed.; *Mechanisms in Homogeneous Catalysis. A Spectroscopic Approach*; Wiley-VCH: Weinheim, 2005.

(4) (a) Basolo, F. *J. Organomet. Chem.* **1990**, *383*, 579. (b) O'Connor, J. M.; Casey, C. P. *Chem. Rev.* **1987**, *87*, 307.

(5) Jordan, R. B. *Reaction Mechanisms of Inorganic and Organometallic Systems*; Oxford University Press: New York, 1998; p 138.

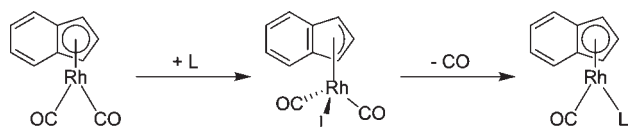
(6) Schuster-Woldan, H. G.; Basolo, F. *J. Am. Chem. Soc.* **1966**, *88*, 1657.

(7) Ji, L.-N.; Rerek, M. E.; Basolo, F. *Organometallics* **1984**, *3*, 740.

(8) (a) Veiros, L. F. *Organometallics* **2000**, *19*, 3127. (b) Calhorda, M. J.; Romão, C. C.; Veiros, L. F. *Chem.—Eur. J.* **2002**, *8*, 868.

(9) (a) Ji, L.-N.; Kershner, D. L.; Basolo, F. *J. Organomet. Chem.* **1985**, *296*, 83. (b) Kershner, D. L.; Rheingold, A. L.; Basolo, F. *Organometallics* **1987**, *6*, 196. (c) Kershner, D. L.; Basolo, F. *J. Am. Chem. Soc.* **1987**, *109*, 7396.

Scheme 1



analogue.^{9b} Basolo and co-workers convincingly established that CO displacement from the pyrrole complex proceeded by an associative mechanism by way of the 18 electron (η^3 -C₄H₄N)Mn(CO)₃(PR₃) ring slip intermediate. Because of the presence of the electron withdrawing nitrogen atom, the η^3 intermediate was proposed to be more energetically accessible than the equivalent carbocyclic complex. Furthermore, by employing substituted *N*-heterocycles such as 2,5 dimethyl- and 3,4 dimethyl pyrrole, it was established that in the pyrrole system, the nitrogen atom was contained within the allylic system of the η^5 intermediate.^{9b,c} We were interested in determining whether such mechanistic generalizations for the *N*-heterocyclic relative to the carbocyclic systems could be made in the displacement of ligands that, unlike CO, are weakly coordinated to transition metal centers. For example, would substitution of Solv from (η^5 -C₄H₄N)Mn(CO)₂(Solv) also demonstrate rate enhancement relative to CpMn(CO)₂(Solv) when Solv is a weakly coordinated solvent or solute present in large excess (Scheme 2)?

Addressing this issue is important since ring slipped or lower hapticity organometallic intermediates are often invoked in catalytic and stoichiometric reactions.^{4b,10} In several such homogeneous reactions, the solvent is weakly coordinated to the metal center, and establishing the possible accessibility of a ring slipped intermediate in the displacement of the solvent is important.¹¹

We report in this paper a comparison between the reactivity of the (η^5 -DMP)Mn(CO)₂(Solv) [DMP = 2,5 dimethylpyrrole] and CpMn(CO)₂(Solv) complexes [Solv = cyclohexane (CyH), η^2 -benzene (Bz), 1-bromohexane (Br-hex), tetrahydrofuran (THF), and η^2 -cyclooctene]. These solvents were chosen because of their different binding strengths to the Mn center, spanning a range from ~8 to 34 kcal/mol.¹² Furthermore, comparison of the reactivity differences between the *N*-heterocyclic and carbocyclic systems is facilitated since the displacement of these solvents from CpMn(CO)₂ has already been investigated.¹² Given the large range of reaction time scales, a variety of time-resolved infrared techniques were employed to include step-scan, rapid-scan FTIR, and laser flash photolysis. In addition, DFT calculations were performed on all the complexes to

lend support for the experimental findings. Surprisingly, unlike the displacement of CO from the related complexes, rate enhancement was not observed in the case of relatively weakly coordinated ligands. However, both associative (ring slip) and dissociative channels are predicted to contribute to the displacement of the stronger η^2 bound cyclooctene from the (η^5 -DMP)Mn(CO)₂ fragment.

Experimental and Theoretical Methods

Kinetic experiments were performed using a Bruker Vertex 80 FTIR with step-scan and rapid-scan capabilities. Sample photolysis was conducted using the third harmonic (355 nm) of a Continuum Surelite I-10 Nd:YAG laser operating at 1 Hz. A syringe pump was used to flow solution through a temperature controlled 0.5 mm path length IR cell with CaF₂ windows (Harrick Scientific) to ensure that a fresh solution was photolyzed with every shot of the laser. The temperature was monitored by a thermocouple located close to the photolysis solution and maintained by a water circulator to within ± 0.1 °C. All spectra were obtained at 8 cm⁻¹ resolution.

Some experiments were conducted using a flash photolysis apparatus employing infrared detection. The temporal profile of the photogenerated intermediates were probed with infrared light from a water cooled CO probe laser (1600–1920 cm⁻¹). The infrared output was attenuated by absorptive filters (OD = 2.5) prior to merging with the UV photolysis beam. The colinear IR/UV beams were passed through the sample cell following which the UV was split from the IR beam which was detected with a liquid nitrogen cooled MCT detector. The signal was sent to a 1 GHz digital storage oscilloscope for processing.

The photolysis solutions were 3–4 mM in the Mn complex in cyclohexane solvent. To this solution, either benzene, 1-bromohexane or THF was added to yield a 1.12 M, 2.85 and 3.08 M solution in these solvents, respectively. The appropriate amount of incoming ligand, either THF, 2,6-lutidine, or cyclooctene was added prior to photolysis. The reaction rates were studied over a 30 K temperature range.

Longer time scale kinetic experiments involving the Mn-(η^2 -cyclooctene) complexes were conducted by photolyzing an 11.0 mL solution of the parent tricarbonyl (~4 mM) in *n*-heptane solvent in the presence of 0.70 M cyclooctene under Ar. To the resulting solution containing the Mn-(η^2 -cyclooctene) complex the appropriate amounts of 2-picoline and *n*-heptane were added, and the solution was heated to the required temperature (358 K). IR spectra were subsequently obtained at known time intervals.

All experiments were conducted under pseudo first order conditions. Observed rate constants (k_{obs}) were determined from a first order fit to the absorbance versus time profile of either the reactant or the product complexes. Activation parameters were calculated from the temperature dependence of the second order rate constants obtained from the k_{obs} versus [L] plots. Errors in the kinetic parameters were obtained from linear fits to the data as reported by the data analysis program Kaleidagraph.

The (η^5 -DMP)Mn(CO)₃ and CpMn(CO)₂(η^2 -cyclooctene) complexes were synthesized according to literature procedures.^{9c,12f} The CpMn(CO)₂(η^2 -cyclooctene) complex had a small amount of parent tricarbonyl present, and since this complex is thermally unreactive the product was not purified further. The DMP complex was relatively unstable in solution at room temperature and was therefore synthesized, isolated as a yellow oil, dissolved in cyclohexane, and the resulting solution frozen. The frozen solutions were stable for several weeks. All solvents and reagents were anhydrous grade and of >99% purity (Aldrich) and used as received. 2-Picoline was freshly distilled under a nitrogen atmosphere,

(10) (a) Marder, T. B.; Roe, D. C.; Milstein, D. *Organometallics* **1988**, *7*, 1451. (b) Borrini, A.; Diversi, P.; Ingrosso, G.; Lucherini, A.; Serra, G. *J. Mol. Catal.* **1985**, *30*, 181. (c) Bonnemann, H. *Angew. Chem., Int. Ed. Engl.* **1985**, *24*, 248. (d) Foo, T.; Bergman, R. G. *Organometallics* **1992**, *11*, 1801. (e) Schmid, M. A.; Alt, H. G.; Milius, W. *J. Organomet. Chem.* **1996**, *514*, 45. (f) Llinas, G. H.; Day, R. O.; Rausch, M. D.; Chien, J. C. W. *Organometallics* **1993**, *12*, 1283. (g) Garrett, C. E.; Fu, G. C. *J. Org. Chem.* **1998**, *63*, 1370. (h) McFarlane, K. L.; Lee, B.; Fu, W.; van Eldik, R.; Ford, P. C. *Organometallics* **1998**, *17*, 1826. (i) Chin, R. M.; Baird, B.; Jarosh, M.; Rassman, S.; Barry, B.; Jones, W. D. *Organometallics* **2003**, *22*, 4829.

(11) Wax, M. J.; Bergman, R. G. *J. Am. Chem. Soc.* **1981**, *103*, 7028.

(12) (a) Lugovskoy, S.; Schultz, R. H. *Dalton Trans.* **2003**, 3103. (b) Bengali, A. A.; Abdulrazak, K. T.; Fan, W. Y. *Organometallics* **2009**, *28*, 3123. (c) Bengali, A. A. *Organometallics* **2000**, *19*, 4000. (d) Bengali, A. A.; Fan, W. Y. *Organometallics* **2008**, *27*, 5488. (e) Coleman, J. E.; Dulaney, K. E.; Bengali, A. A. *J. Organomet. Chem.* **1999**, *572*, 65. (f) Angelici, R. J.; Loewen, W. *Inorg. Chem.* **1967**, *6*, 682.

Scheme 2

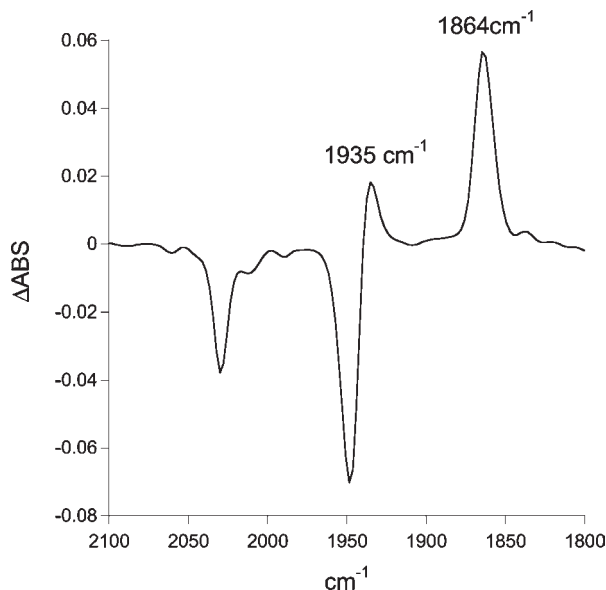
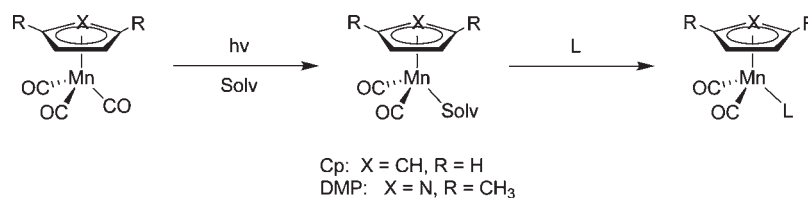


Figure 1. Difference spectra obtained upon photolysis of a cyclohexane solution of $(\eta^5\text{-DMP})\text{Mn}(\text{CO})_3$ in the presence of THF at 293 K. The positive peaks are due to the formation of the $(\eta^5\text{-DMP})\text{Mn}(\text{CO})_2(\text{THF})$ complex, and the negative peaks are associated with depletion of parent upon photolysis.

and cyclooctene was filtered over neutral alumina prior to use.

The structure, stabilities, and vibrational frequencies of all ground state, transition state, and intermediate complexes were studied using the Gaussian 03 program employing the B3LYP functional.¹³ The transition metal, C, N, H, Br, and O atoms were described by the 6-31G* basis set. Bond dissociation enthalpies (BDEs) were calculated as the difference in enthalpy between the product $\text{XMn}(\text{CO})_2(\text{Solv})$ and the reactant $\text{XMn}(\text{CO})_2 + \text{Solv}$ enthalpies [X = $\eta^5\text{-DMP}$ and Cp]. Transition state structures were modeled based on the studies of Veiros and were confirmed by frequency calculations which showed only one imaginary frequency along the reaction coordinate.^{8a,b}

Results and Discussion

As in the case of the analogous $\text{CpMn}(\text{CO})_3$ system,¹² photolysis of $(\eta^5\text{-DMP})\text{Mn}(\text{CO})_3$ in the presence of solvent yields the appropriate solvated species, $(\eta^5\text{-DMP})\text{Mn}(\text{CO})_2(\text{Solv})$. For example, as shown in Figure 1, the $(\eta^5\text{-DMP})\text{Mn}(\text{CO})_2(\text{THF})$ complex with CO stretching absorbances at 1935 and 1864 cm^{-1} is formed upon photolysis of $(\eta^5\text{-DMP})\text{Mn}(\text{CO})_3$ in the presence of THF. From the change in the intensity of the parent CO bands upon photolysis, the conversion to the solvate complex is estimated to be $\approx 20\%$.

Table 1. CO Stretching Frequencies for the $\text{XMn}(\text{CO})_2(\text{Solv})$ [X = $\eta^5\text{-DMP}$ or Cp] Complexes in Cyclohexane Solvent at 298 K^a

solv	$\nu_{\text{CO, DMP}}$ (cm^{-1})	$\nu_{\text{CO, Cp}}$ (cm^{-1})
cyclohexane	1893	1958, 1891
benzene	1898	1955, 1893
1-bromohexane	1882	1876
tetrahydrofuran	1935, 1864	1931, 1860
cyclooctene	1962, 1902	1959, 1897

^aIn some cases the position of only one band is listed since the remaining band is obscured by the CO absorbance of the parent tricarbonyl.

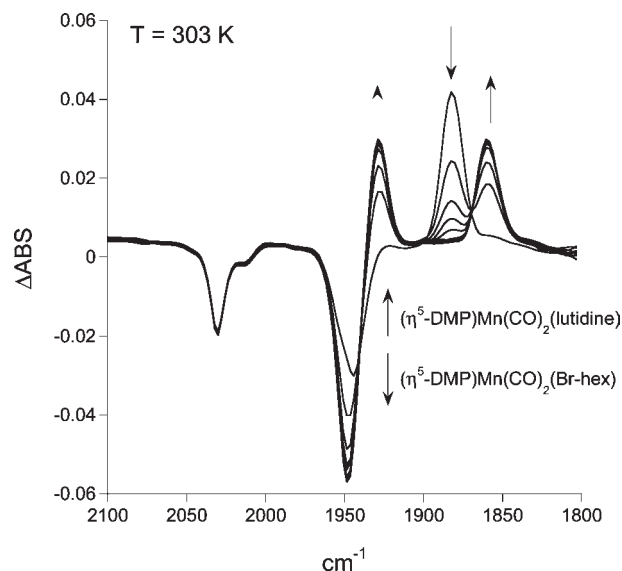


Figure 2. Reaction of the initially formed $(\eta^5\text{-DMP})\text{Mn}(\text{CO})_2(\text{Br-hex})$ complex with 2,6-lutidine in cyclohexane at 303 K. Photolysis was conducted in the presence of [1-bromohexane] = 2.85 M and [2,6-lutidine] = 0.43 M in cyclohexane solution. Spectra were obtained at 600 ms intervals. The ν_{CO} band at 1950 cm^{-1} is a composite of the E vibrational mode of the parent tricarbonyl and the A_1 mode of the Br-hex solvate.

As shown in Table 1, for all solvates studied, the CO stretching frequencies are similar for the DMP and Cp complexes suggesting that the electron density on the Mn center is not significantly affected when the carbocyclic Cp ligand is replaced with DMP. The electron withdrawing tendency of the nitrogen atom is likely offset by the inductive effect of the CH_3 groups resulting in similar donor characteristics for the DMP and Cp ligands.

The reaction of $(\eta^5\text{-DMP})\text{Mn}(\text{CO})_2(\text{Solv})$ with ligand L, shown in Figure 2 in the case of Solv = 1-bromohexane and L = 2,6-lutidine, results in the displacement of the weakly bound solvent molecule to form the $(\eta^5\text{-DMP})\text{Mn}(\text{CO})_2\text{L}$ complex. All substitution reactions studied displayed a linear relationship between k_{obs} and [L], as illustrated by the displacement of CyH from $(\eta^5\text{-DMP})\text{Mn}(\text{CO})_2(\text{CyH})$ by THF shown in Figure 3. The linear behavior of k_{obs} as a

(13) (a) Frisch, M. J. et al. *Gaussian 03*, Revisions B. and B.05; Gaussian, Inc.: Wallingford, CT, 2004. (b) Becke, A. D. *J. Phys. Chem.* **1993**, *98*, 5648. (c) Lee, C.; Yang, W.; Parr, R. G. *Phys. Rev. B* **1988**, *37*, 785.

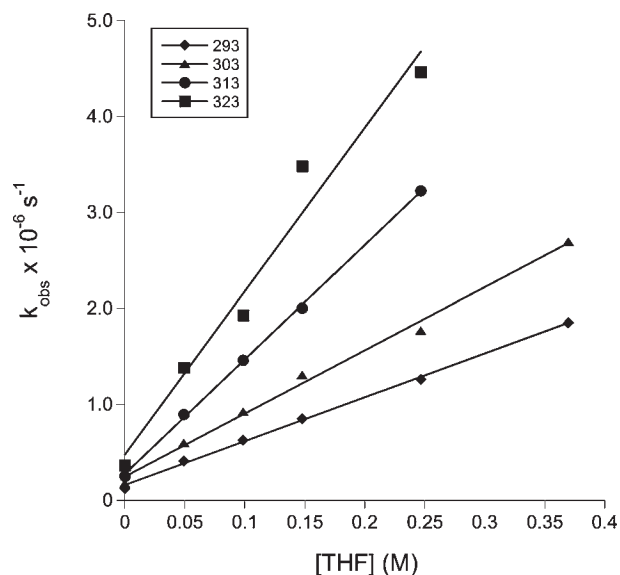


Figure 3. Plot of k_{obs} versus [THF] for the reaction of $(\eta^5\text{-DMP})\text{Mn}(\text{CO})_2(\text{CyH})$ with THF in cyclohexane at several temperatures.

function of [L] does not assist in the assignment of a displacement mechanism since it is consistent with either a dissociative, associative, or interchange pathway.¹⁴ However, as discussed below, the agreement between the activation parameters and the calculated Mn-Solv binding strengths supports a dissociative or I_d mechanism of solvent substitution in all cases.

Unlike what is observed in the Cp system, the k_{obs} versus [L] plots for DMP display significant non-zero intercepts. Experiments performed in the absence of incoming ligand (i.e., [L] = 0) confirmed that the non-zero intercepts are primarily due to the decomposition of the $(\eta^5\text{-DMP})\text{Mn}(\text{CO})_2(\text{Solv})$ complex by an undetermined pathway. For example, at 293 K in the absence of incoming ligand, the $(\eta^5\text{-DMP})\text{Mn}(\text{CO})_2(\text{CyH})$ complex exhibited a single exponential decay with $k_{\text{obs}} = 1.3 \times 10^5 \text{ s}^{-1}$ similar to an intercept of $1.9 \times 10^5 \text{ s}^{-1}$ obtained at this temperature (Figure 3). By contrast, the intercept for the Cp system is smaller by a factor of 4. The larger background decay rate constants for the DMP complexes are probably due to the fact that the η^5 coordinated DMP ligand in the parent tricarbonyl can also act as a nucleophile toward the $(\eta^5\text{-DMP})\text{Mn}(\text{CO})_2(\text{Solv})$ complex.¹⁵ Similar non-zero intercepts were also observed previously for the displacement of CO by $\text{P}(\text{OEt})_3$ from the $(\eta^5\text{-DMP})\text{Mn}(\text{CO})_3$ complex.^{9c} Alternatively, the solvent adduct can react with the parent complex, yielding a dinuclear species with a bridging CO group, as was observed by Poliakov et al. for $\text{CpMn}(\text{CO})_3$.¹⁶ Also, as noted earlier, $(\eta^5\text{-DMP})\text{Mn}(\text{CO})_3$ is inherently more unstable than the analogous carbocyclic complex resulting in a larger background decay rate. On the basis of the data, it is reasonable to conclude that the non-zero intercepts are not due to a parallel solvent displacement pathway.

As shown in Figure 4 and in Table 2, for all the systems studied, the second order rate constants obtained from the

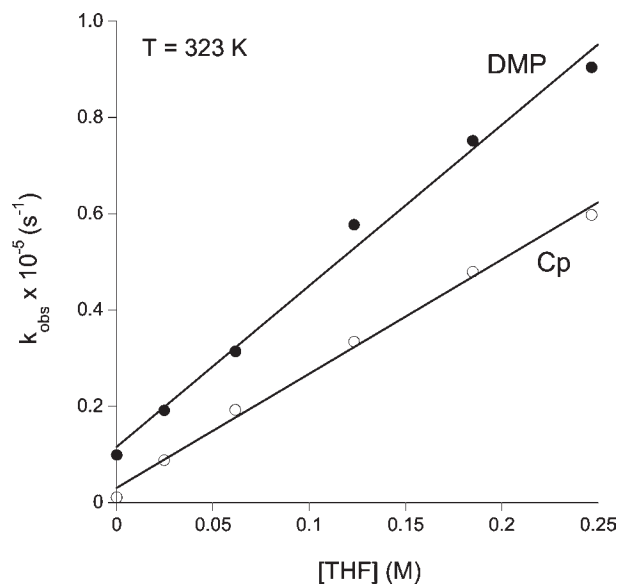


Figure 4. Plot of k_{obs} versus [THF] for the reaction of $\text{XMn}(\text{CO})_2(\eta^2\text{-Bz})$ [$\text{X} = \eta^5\text{-DMP, Cp}$] with THF at 323 K in cyclohexane solvent. The similar slope for the two plots suggests the lack of a significant rate enhancement upon replacement of Cp with the DMP ligand. The intercept for the DMP system is larger than for Cp although, as explained in the text, this does not imply a different displacement mechanism.

slopes of the k_{obs} versus [L] plots are within a factor of 10 for the DMP and Cp systems with very similar activation parameters. These results are in dramatic contrast to the large enhancement in CO substitution rates observed upon replacement of Cp with pyrrole or DMP as the π cyclic ligand.⁹ Since thermal displacement of CO from $\text{CpMn}(\text{CO})_3$ is not observed, the rate enhancement cannot be quantified. However, given the fact that CO substitution occurs within hours from the DMP complex at elevated temperatures while in the case of $\text{CpMn}(\text{CO})_3$ no substitution occurs for days, the rate enhancement is significant. In early studies, Basolo estimates a $10^6\text{--}10^8$ fold rate enhancement.^{9b} As shown in Table 2, theoretical calculations demonstrate that the Mn-Solv binding strength is unaffected by replacement of the Cp carbocycle with the heterocyclic DMP ligand. Since previous studies have shown that displacement of solvent by an incoming ligand follows either a dissociative or an I_d pathway for many $\text{CpMn}(\text{CO})_2\text{Solv}$ complexes,¹² the almost identical activation parameters and calculated Mn-Solv binding strengths indicate a similar substitution mechanism for the DMP system. The data therefore point to a lack of $\eta^5 \rightarrow \eta^3$ ring slippage in the displacement of solvent from $(\eta^5\text{-DMP})\text{Mn}(\text{CO})_2(\text{Solv})$.

These results are in marked contrast to earlier work by Basolo which provided convincing evidence for an associative $\eta^5 \rightarrow \eta^3$ ring slip mechanism for the substitution of CO from $(\eta^5\text{-C}_4\text{H}_4\text{N})\text{Mn}(\text{CO})_3$ and $(\eta^5\text{-DMP})\text{Mn}(\text{CO})_3$.⁹ Thus for example, the observed activation enthalpy of 26.5 kcal/mol for the displacement of CO from $(\eta^5\text{-DMP})\text{Mn}(\text{CO})_3$ by $\text{P}(\text{OEt})_3$ is considerably less than the calculated Mn-CO bond strength of 55 kcal/mol. The primary difference between the CO and the Solv displacement reactions is that the Mn-Solv binding enthalpies ranging from 10 to 25 kcal/mol are considerably weaker than the Mn-CO interaction. Thus, if the transition state for the $\eta^5 \rightarrow \eta^3$ hapticity shift is higher in energy than the strength of the weak $(\eta^5\text{-DMP})\text{Mn}(\text{CO})_2\text{-Solv}$ bond, a dissociative pathway will be accessed and rate

(14) Schultz, R. H. *Int. J. Chem. Kinet.* **2004**, *36*, 427.

(15) Pyshnograeva, N. I.; Setkina, V. N.; Andrianov, V. G.; Struchkov, Yu. T.; Kursanov, D. N. *J. Organomet. Chem.* **1978**, *157*, 431.

(16) Creaven, B. S.; Dixon, A. J.; Kelly, J. M.; Long, C.; Poliakov, M. *Organometallics* **1987**, *6*, 2600–2605.

Table 2. Comparison of the Kinetic Parameters for the DMP and Cp Systems^a

Solv/L	$k_{\text{DMP}}/k_{\text{Cp}}$	$(\eta^5\text{-DMP})\text{Mn}(\text{CO})_2(\text{Solv})$			$\text{CpMn}(\text{CO})_2(\text{Solv})$		
		ΔH^\ddagger (kcal/mol)	BDE ^b (kcal/mol)	ΔS^\ddagger (e.u)	ΔH^\ddagger (kcal/mol)	BDE ^b (kcal/mol)	ΔS^\ddagger (e.u)
CyH/THF	3.7	7.8 ± 0.7	7.4	-1.0 ± 2.0	7.2 ± 0.6 ^c	7.6	-6.2 ± 3.5 ^c
Bz/THF	1.6	14.9 ± 1.4	13.6	+12.5 ± 4.5	14.8 ± 1.4	11.1	+11.7 ± 5.0
Br-hex/lutidine	0.4	21.1 ± 0.4	24.7	+11.8 ± 1.0	18.3 ± 0.6	24.7	+4.2 ± 1.0
THF/cyclooctene	0.1	22.1 ± 0.5	25.5	+5.5 ± 1.5	23.4 ± 2.0 ^d	25.9	+17.7 ± 5.0 ^d
CO/P(OEt) ₃	~ 10 ⁶	26.4 ± 0.8 ^e	54.9	-19.4 ± 1.0 ^e		55.2	

^a For a given solvent (Solv) and incoming ligand (L) the slopes of the k_{obs} versus [L] plots were used to determine the ratio, $k_{\text{DMP}}/k_{\text{Cp}}$, at 293 K. In all cases the relative rate constants for a given solvate were obtained with the same incoming ligand L. ^b Calculated values. ^c Ref 12a. ^d Ref 12e. ^e Ref 9c.

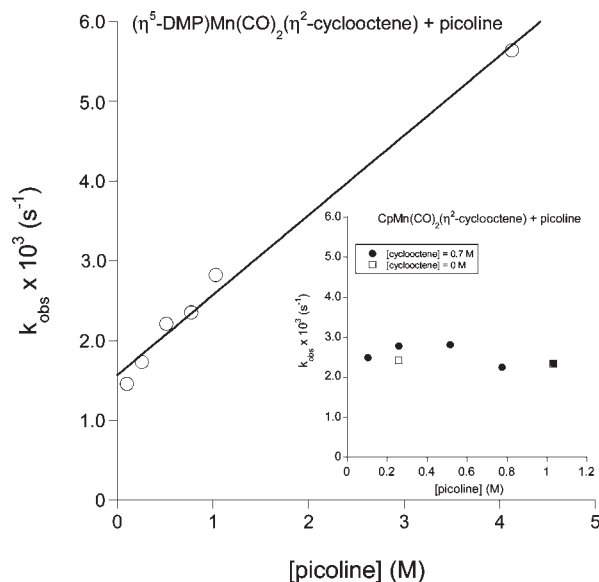
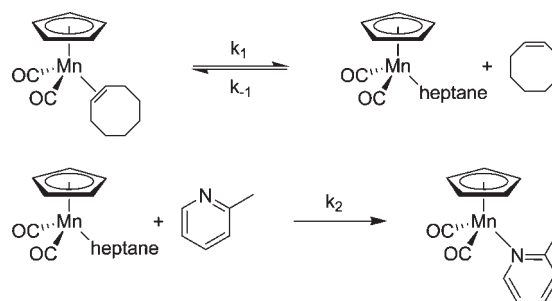


Figure 5. Plot of k_{obs} versus [2-picoline] at 358 K for the displacement of cyclooctene from the DMP and Cp complexes by 2-picoline in heptane. Note that while the plot is linear for the DMP system, as shown in the inset, k_{obs} does not vary with [2-picoline] for the Cp complex.

enhancement relative to the Cp system will not be observed. While ΔH^\ddagger for a dissociative process should be less than the BDE, the correlation between ΔH^\ddagger and BDE is always evident. For the $(\eta^5\text{-DMP})\text{Mn}(\text{CO})_3$ complex, the η^3 transition state enthalpy is lower than the calculated 55 kcal/mol Mn-CO BDE (vide infra) and therefore rate enhancement is observed.

In an attempt to determine the lower limit of the Mn-Solv binding enthalpy when rate enhancement may be observed, we chose to study the displacement of the more strongly bound cyclooctene ligand from the Cp and DMP complexes. The experimentally determined^{12f} BDE of 34.9 kcal/mol for the $\text{CpMn}(\text{CO})_2(\eta^2\text{-cyclooctene})$ interaction is intermediate between the calculated value of 52–55 kcal/mol for the Mn-CO BDE¹⁷ when rate enhancement is observed and 24 kcal/mol for the Mn-THF BDE^{12e} when it is not.

Unlike the other solvents, important differences in the mechanism of substitution of the η^2 bound cyclooctene ligand from the DMP and Cp systems are observed. As shown in Figure 5, a plot of k_{obs} versus [2-picoline] is linear for the DMP system while for the carbocyclic analogue, k_{obs} does not vary with [2-picoline]. This observation points to a difference in the mechanism of alkene substitution from the Mn center. The invariance of k_{obs} with ligand concentration

Scheme 3

in the case of the Cp complex suggests that a dissociative mechanism is operative with the disruption of the $\text{CpMn}(\text{CO})_2(\eta^2\text{-cyclooctene})$ bond as the rate limiting step (Scheme 3).

Previous studies by Angelici and Loewen have convincingly demonstrated that displacement of a variety of alkenes, including cyclooctene, from the $\text{CpMn}(\text{CO})_2(\eta^2\text{-alkene})$ complexes follow a dissociative mechanism.^{12f} Our results are therefore not surprising. The $\text{CpMn}(\text{CO})_2(\text{heptane})$ complex is a likely intermediate since it has been observed previously.¹⁸ Applying the steady state assumption yields,

$$k_{\text{obs}} = \frac{k_1}{\frac{k_{-1}}{k_2} \left\{ \frac{[\text{cyclooctene}]}{[\text{picoline}]} \right\} + 1} \quad (1)$$

In the current experiments, [cyclooctene]/[2-picoline] was varied from 7 to 0.7. The observed lack of k_{obs} dependence on [2-picoline] can therefore be explained if $k_{-1}/k_2 < 0.1$. Under these conditions, k_{obs} will approach a limiting value of k_1 and will be insensitive to the [2-picoline] as observed. A ratio of 0.1 is not unreasonable since previous studies have demonstrated that the related complex $\text{CpMn}(\text{CO})_2(\text{cyclohexane})$ reacts with cyclopentene 3–4 times slower than with pyrrolidine, corresponding to a k_{-1}/k_2 ratio of 0.25.^{12a} Also, the reaction of $\text{CpMn}(\text{CO})_2(\text{heptane})$ with silanes was found to be as much as nine times slower than with PPh_3 ($k_{-1}/k_2 \approx 0.1$).¹⁹ Thus, the average value of $2.5 \pm 0.3 \times 10^{-3} \text{ s}^{-1}$ for k_{obs} at 358 K can be assigned to k_1 in good agreement with a previously reported value of $1.93 \times 10^{-3} \text{ s}^{-1}$ at 353 K.^{12f} To further confirm this interpretation of the kinetic results and to establish the value of k_1 under present experimental conditions, the $\text{CpMn}(\text{CO})_2(\eta^2\text{-cyclooctene})$ complex was isolated and its reaction with 2-picoline studied with

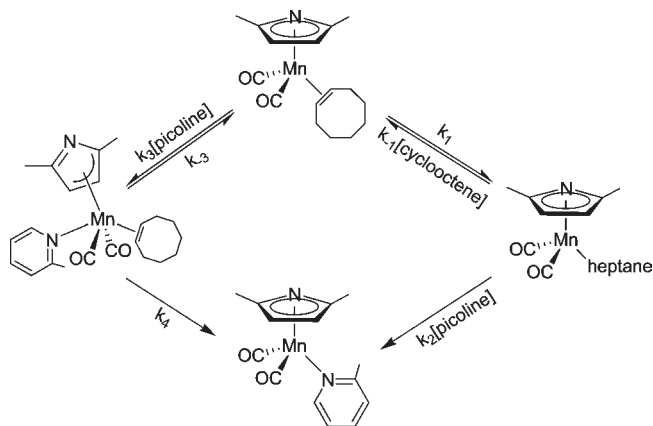
(18) Yang, P.-F.; Yang, G. K. *J. Am. Chem. Soc.* **1992**, *114*, 6937.

(19) Hester, D. M.; Sun, J.; Harper, A. W.; Yang, G. K. *J. Am. Chem. Soc.* **1992**, *114*, 5234.

Table 3. Calculated Enthalpic Parameters for the Reaction: $(\eta^5\text{-DMP})\text{Mn}(\text{CO})_2\text{(Solv)} + \text{L} \rightarrow (\eta^3\text{-DMP})\text{Mn}(\text{CO})_2\text{L}^a$

Solv/L	$\eta^3\text{-TS}$ (kcal/mol)	$\eta^3\text{-I}$ (kcal/mol)	Mn-Solv BDE (kcal/mol)
THF/C ₂ H ₄	29.2	22	25.5
C ₂ H ₄ /pyridine	28.4		31.8

^aThe enthalpy of the associative transition state ($\eta^3\text{-TS}$) and η^3 intermediate ($\eta^3\text{-I}$) for two Solv/L combinations along with the Mn-Solv binding enthalpies are presented.

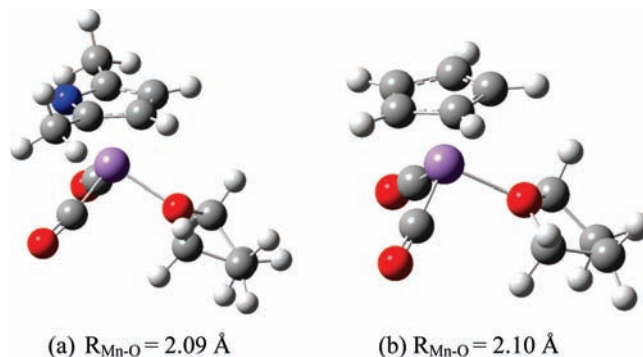
Scheme 4

[cyclooctene] = 0 M. According to eq 1, $k_{\text{obs}} = k_1$ under these conditions. Values of $2.4 \times 10^{-3} \text{ s}^{-1}$ and $2.3 \times 10^{-3} \text{ s}^{-1}$ were obtained for k_{obs} with [2-picoline] = 0.25 and 1.0 M, respectively. The agreement between this value of k_1 and that obtained from the in situ experiments in the presence of both cyclooctene and 2-picoline provides confirmation that the invariance of k_{obs} upon [2-picoline] is due to the saturation of the rate constant under the conditions of the experiment.

In contrast to the Cp system, k_{obs} for the displacement of η^2 cyclooctene from the $(\eta^5\text{-DMP})\text{Mn}(\text{CO})_2$ fragment increases linearly with [2-picoline]. The theoretical calculations detailed below (Table 3) suggest that in the case of Solv = cyclooctene, the enthalpy of the η^3 associative transition state is similar to the Mn- $(\eta^2\text{-cyclooctene})$ binding enthalpy. Thus, it is reasonable to suggest that both associative and dissociative channels are accessible for the substitution of cyclooctene from the DMP complex. The overall reaction mechanism is presented in Scheme 4. Applying the steady state assumption to the intermediate $(\eta^5\text{-DMP})\text{Mn}(\text{CO})_2(\text{heptane})$ and $(\eta^3\text{-DMP})\text{Mn}(\text{CO})_2(\eta^2\text{-cyclooctene})(2\text{-picoline})$ complexes, and further assuming that $k_{-1} < k_2$ as discussed for the Cp system, yields the k_{obs} versus [2-picoline] dependence shown in eq 2. Thus, a plot of k_{obs} versus [2-picoline] should be linear with a non-zero intercept yielding k_1 , as observed in Figure 5.

$$k_{\text{obs}} = k_1 + \frac{k_3 k_4 [\text{picoline}]}{k_{-3} + k_4} \quad (2)$$

As discussed earlier, the k_{obs} versus [L] plots for the DMP systems tend to have non-zero intercepts because of the higher background decay rate of the complexes. However, unlike the other solvents, for Solv = cyclooctene, the background decay rate obtained in the absence of incoming ligand was 16 times less than the intercept of the k_{obs} versus [cyclooctene] plot. This observation suggests that the non-zero intercept is not primarily due to the decomposition of the

**Figure 6.** Calculated structures for the (a) $(\eta^5\text{-DMP})\text{Mn}(\text{CO})_2\text{THF}$ and (b) $\text{CpMn}(\text{CO})_2\text{THF}$ molecules. The geometries and THF binding strengths are similar for both complexes.

$(\eta^5\text{-DMP})\text{Mn}(\text{CO})_2(\eta^2\text{-cyclooctene})$ complex, but rather is evidence for the presence of another substitution pathway. Importantly, the k_1 value of $1.6 \pm 0.1 \times 10^{-3} \text{ s}^{-1}$ for the DMP system is similar to that of the Cp complex. This agreement is consistent with the expectation that the binding enthalpies of the $\eta^2\text{-cyclooctene}$ solvent are not likely to differ for the two complexes.

The kinetic results for the DMP system are therefore consistent with concurrent associative and dissociative channels for the displacement of η^2 coordinated cyclooctene by 2-picoline. Importantly, while the overall substitution mechanism differs when Cp is replaced with DMP, there is no rate enhancement since the activation enthalpies for the associative and dissociative pathways are similar in the latter case. The data obtained in the current investigation suggests that for the $(\eta^5\text{-DMP})\text{Mn}(\text{CO})_2(\text{Solv})$ systems, the transition from a dissociative to associative substitution pathway occurs when the activation barrier approaches ~ 33 kcal/mol, the binding enthalpy of cyclooctene to the Mn center. Thus, this value can be assigned to the enthalpic cost required to both disrupt the aromaticity of the pyrrole ligand and expand the coordination number on the Mn center to accommodate the incoming ligand as the η^3 intermediate is formed. Rate enhancement relative to the Cp system is therefore expected only for the displacement of ligands that are bound to the Mn center by more than 33 kcal/mol. In such cases, the ring slipped transition state is predicted to be more energetically accessible than the dissociative one leading to an increase in the substitution rate. To gain a better understanding of the systems involved and to provide supporting evidence for the experimental results, DFT calculations were performed on the relevant compounds.

Theoretical Modeling

The binding strengths of various solvents to the metal center in the $\text{CpMn}(\text{CO})_2$ and $(\eta^5\text{-DMP})\text{Mn}(\text{CO})_2$ fragments are presented in Table 2. Good agreement with the experimental values suggests the level of theory applied is appropriate for modeling the systems under investigation. The calculated geometries for a typical solvated complex are shown in Figure 6 for the $\text{CpMn}(\text{CO})_2\text{THF}$ and $(\eta^5\text{-DMP})\text{Mn}(\text{CO})_2\text{THF}$ molecules. The results indicate that replacement of Cp with the DMP ligand does not affect either the strength of the Mn-Solv bond or the geometry of the solvated complex. These results are consistent with the observation that the CO stretching vibrations of the DMP

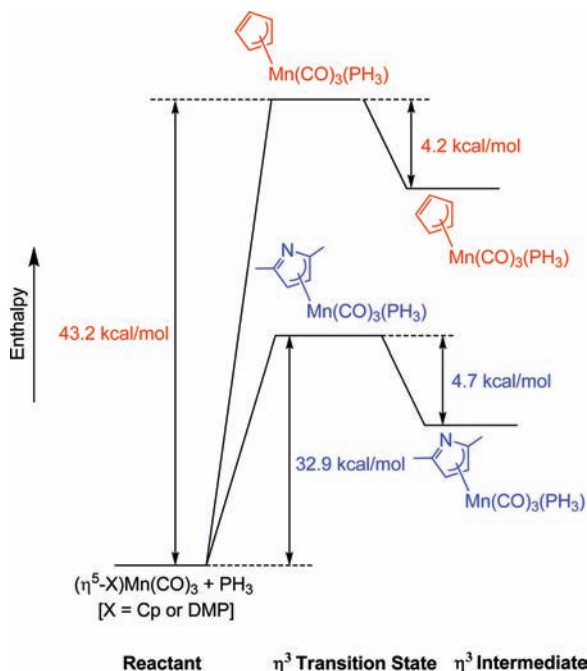


Figure 7. Enthalpy diagram for the displacement of CO from $(\eta^5\text{-X})\text{Mn}(\text{CO})_3 + \text{PH}_3$ where $\text{X} = \text{Cp}$ and DMP. The η^3 transition state is energetically more accessible for the DMP system.

and Cp complexes are nearly identical, suggestive of similar electron density on both metal centers.

The enthalpies of transition states and intermediates for some $\eta^5 \rightarrow \eta^3$ ring slipped reactions were calculated for the Cp and DMP complexes. The most favorable η^3 transition state structure for the DMP system is one in which the nitrogen atom is not part of the allylic system, consistent with the enhanced steric bulk because of the presence of the CH_3 groups at the 2,5 positions. However, the calculated difference in enthalpy between the structures with and without nitrogen participation in the allylic system is < 1.0 kcal/mol, and the two isomers can therefore be considered as isoenergetic.

The modeling results shown in Figure 7 are consistent with the experimental data. For example, in the reaction of $\text{CpMn}(\text{CO})_3$ with PH_3 , the ring slipped transition state, $(\eta^3\text{-Cp})\text{Mn}(\text{CO})_3\text{PH}_3$, is 43 kcal/mol higher than the ground state. By contrast, in the DMP system the η^3 transition state is energetically more accessible at 32.9 kcal/mol. Interestingly, this activation enthalpy is similar to the calculated value of 30 kcal/mol for the η^3 transition state accessed in the displacement of CO from the $(\eta^5\text{-Indenyl})\text{Mn}(\text{CO})_3$ complex by PH_3 .^{8a} Importantly, the associative transition state for the DMP complex is significantly lower in energy relative to the 54.9 kcal/mol Mn-CO BDE. It is therefore not surprising that substitution of CO from the DMP complex proceeds by an associative mechanism and shows a significant rate enhancement relative to the Cp system. The η^3 transition state energy for the DMP complex compares favorably to the experimental value of 26.4 kcal/mol for the displacement of CO by $\text{P}(\text{OEt})_3$.^{9c} However, when $\text{P}(n\text{-Bu})_3$ was used as the incoming ligand, an activation barrier of 15.7 kcal/mol was reported.

The enthalpic profiles for the weakly solvated complexes studied here have the same basic characteristics. For example, displacement of THF by C_2H_4 (model for cyclooctene used in the experiments) by a ring slip pathway demonstrates

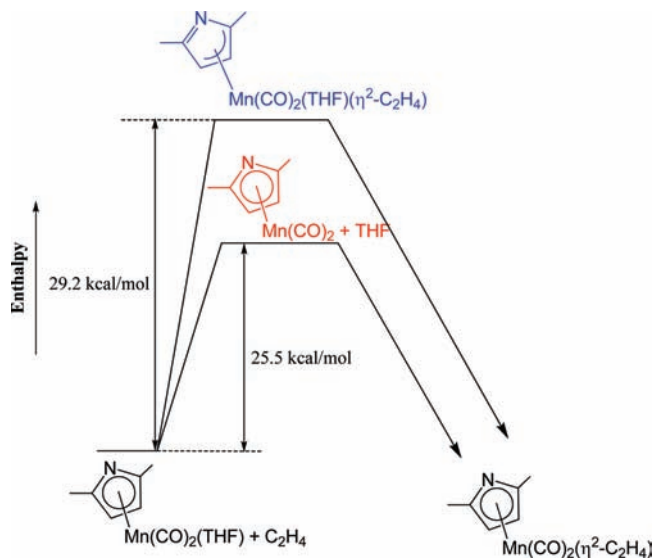


Figure 8. Enthalpy profile for the substitution of THF from the $(\eta^5\text{-DMP})\text{Mn}(\text{CO})_2$ fragment by C_2H_4 . Unlike CO displacement, the dissociative channel for THF substitution has a lower enthalpy than the associative pathway.

a relatively more accessible enthalpic profile for DMP versus Cp. Importantly however, as shown in Figure 8, the key difference from the CO substitution profile is that even for DMP, the η^3 transition state at 29.2 kcal/mol is higher in energy than the calculated value of 25.5 kcal/mol for the Mn-THF bond dissociation enthalpy. Consequently, the lower energy dissociative channel is utilized for the substitution of THF. Since the Mn-THF binding strength remains virtually unaffected when DMP is replaced by Cp, rate enhancement is not observed.

The structures of the η^3 transition state and intermediate are shown in Figure 9. The 2.11 Å Mn-O bond distance in the transition state is similar to that found in the ground state structure (2.09 Å). Furthermore, the incoming C_2H_4 ligand is loosely associated with the metal center as evident by the relatively long 2.82 Å bond distance between the center of the π bond and Mn. Taken together these bond distances suggest there is relatively little bond breaking and making in the transition state. Thus, the higher enthalpy of the transition state relative to the ground state is primarily due to the electronic and structural deformation of the DMP ligand as it undergoes a $\eta^5 \rightarrow \eta^3$ haptotropic shift.

As shown in Table 3, unlike THF, the calculations suggest that for Solv = ethylene, the transition state energies for the associative and dissociative channels are similar. In the $(\eta^5\text{-DMP})\text{Mn}(\text{CO})_2(\eta^2\text{-C}_2\text{H}_4) + \text{pyridine}$ system, the η^3 transition state is predicted to lie 28.4 kcal/mol higher than the ground state while the Mn- $(\eta^2\text{-C}_2\text{H}_4)$ binding enthalpy is calculated to be only ~ 3 kcal/mol higher at 31.8 kcal/mol. Consequently, for the cyclooctene system, it is reasonable to suggest that both substitution channels are accessed in the displacement reaction. As discussed earlier, the kinetic data are consistent with this prediction. Since the transition state enthalpies for the two pathways are calculated to be similar, rate enhancement relative to the Cp system is not observed.

Despite the variation in the solvent/ligand combinations, the activation enthalpies of the corresponding η^3 transition states are similar at 28.4, 29.2, and 32.9 kcal/mol for the $\text{C}_2\text{H}_4/\text{pyridine}$, THF/ C_2H_4 , and CO/ PH_3 systems, respectively.

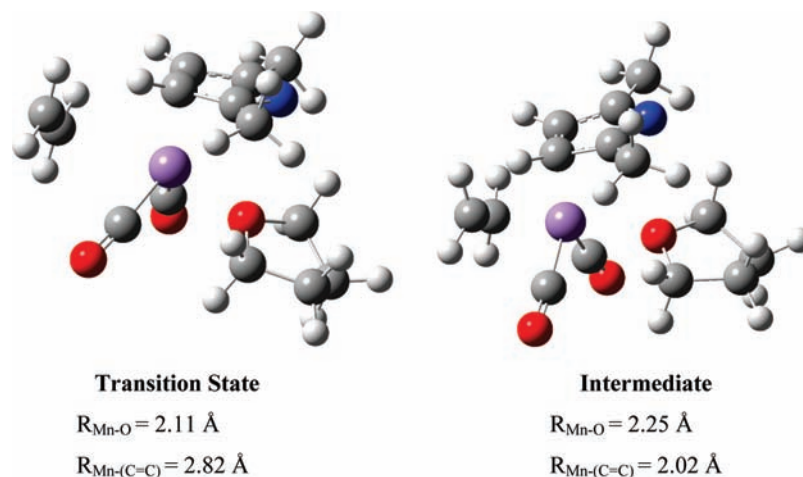


Figure 9. Calculated structures of the $(\eta^3\text{-DMP})\text{Mn}(\text{CO})_2(\text{THF})(\text{C}_2\text{H}_4)$ transition state and intermediate.

Consistent with the experimental results, the similar activation enthalpies suggest that the η^3 transition state is accessible for the displacement of solvents with Mn-Solv BDEs in excess of ~ 33 kcal/mol. Rate enhancement is therefore not expected for weaker bound solvents.

Conclusions

The results of the kinetic study demonstrate that for the $(\eta^5\text{-DMP})\text{Mn}(\text{CO})_2(\text{Solv})$ complexes, the associative $\eta^5 \rightarrow \eta^3$ ring slip substitution pathway becomes competitive with the dissociative channel only when the Mn-Solv bond dissociation enthalpy is > 33 kcal/mol. Thus, unlike CO substitution, rate enhancement relative to the Cp system is not observed in the displacement of weakly bound solvents. For these solvents, the close agreement between the calculated BDEs and the activation enthalpies suggest that the solvent displacement for both the DMP and the Cp complexes proceeds by a dissociative or I_d mechanism. While for the stronger bound cyclooctene ligand rate enhancement is not observed, experimental evidence supported by theoretical calculations demonstrates the accessibility of both dissociative *and* associative substitution channels.

(20) In initial experiments no significant rate enhancement was observed for the substitution of THF or 1-bromohexane from $(\eta^5\text{-Fluorenyl})\text{Mn}(\text{CO})_2(\text{Solv})$.

Previous theoretical studies have calculated a 30 kcal/mol barrier for the $\eta^5 \rightarrow \eta^3$ ring slip of the indenyl ligand in the displacement of CO from $(\eta^5\text{-Indenyl})\text{Mn}(\text{CO})_3$ by PH_3 .^{8a} This activation energy is similar to that of the DMP complex (32.9 kcal/mol) and suggests that substitution of weakly coordinated solvents from the indenyl complexes will display the same characteristics as observed for the DMP system.²⁰

The results of the present study demonstrate that caution must be exercised when extrapolating the results of experiments that provide evidence for an associative ring slip pathway in ligand substitutions. Systems that demonstrate rate enhancement for the substitution of strongly coordinated ligands may not show the same effect for weaker bound substrates.

Acknowledgment. This research was supported by a National Priorities Research Program (NPRP) grant from the Qatar National Research Fund (Grant no. 8-6-7-1). The authors would also like to acknowledge Dr. Jeremy Andreatta for his assistance in conducting some preliminary experiments.

Supporting Information Available: Tables of rate constants for all the systems investigated together with activation parameters. This material is available free of charge via the Internet at <http://pubs.acs.org>.